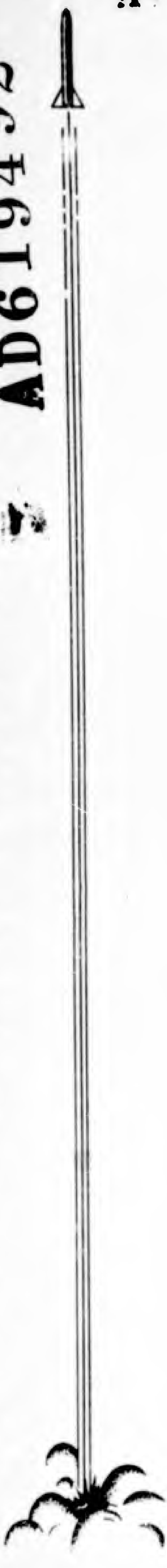

OFFICE OF AEROSPACE RESEARCH
TECHNICAL REPORT

Contract AF 49(638)-1197

TRACE SPECIES IN COMBUSTION GASES
The Formation of Sodium Metaborate

David Fleischer

51 P

AIR FORCE OFFICE OF SCIENTIFIC RESEARCH
WASHINGTON 25, D. C.

November 1964

Thiokol
CHEMICAL CORPORATION
REACTION MOTORS DIVISION
DENVILLE, NEW JERSEY

THIOKOL CHEMICAL CORPORATION
REACTION MOTORS DIVISION

SOLID PROPELLANT TRACING METHODS

David Fleischer

RMD Report 5510-F

November 1964

Approved by: David Burgess
D. S. Burgess
Manager, Physics Department

D J Mann
D. J. Mann
Director of Research

AIR FORCE OFFICE OF SCIENTIFIC RESEARCH
OFFICE OF AEROSPACE RESEARCH
WASHINGTON 25, D. C.

FOREWORD

This is the (approval copy of the)* Final Technical Report under Contract AF 49(638)-1197, covering the period 15 October 1963 - 14 October 1964. This work was performed under the cognizance of the Air Force Office of Scientific Research, Office of Aerospace Research, Washington 25, D. C.

The experimental portion of this program was performed by Mr. Charles McAndrew.

---

* To be deleted in final version.

ABSTRACT

The equilibrium constant for the reaction

$$NaCl(g) + HBO_2(g) = NaBO_2(g) + HCl(g)$$

is determined to be, $K_p = 2.50$ (1980°K). Sodium vapor and boron trichloride (BCl_3) are reacted in a hydrocarbon-air flame contained in a tunnel burner. Conditions are such that the concentrations of HBO_2 and HCl are equal to the total flows of boron and chlorine. The concentration of unreacted sodium is found by line absorption, using an experimentally determined absorption coefficient. The relative contribution of NaCl and $NaBO_2$ to the chemically combined sodium concentration can be assessed by removing the direct proportionality between chlorine and boron flows. This is done by adding chlorine, beyond that present in the BCl_3. The H-atom concentration is also required, and is inferred from the intensity of the $^2\Pi \rightarrow {}^2\Sigma$ (0, 0) OH-band.

TABLE OF CONTENTS

TABLES

FIGURES

INTRODUCTION

Trace metal species can influence the electrical and optical properties of combustion gases out of all proportion to their concentrations. The interpretation of such effects requires a knowledge of how the total metal concentration is distributed among its various compounds in the combustion gas, but the thermochemical data required to calculate such distributions is often not available.

A method for directly determining such data is the evaluation of an equilibrium constant, for a reaction in which only the free energy of formation of the desired species is unknown. The standard free energy change and the equilibrium constant for the reaction

$$M + AB = MB + A \tag{1}$$

are related by

$$\Delta F^{o} = - RT \ln K = - RT \ln \frac{(MB)(A)}{(M)(AB)} \tag{2}$$

The desired quantity, the free-energy of formation (ΔF_f) of MB then follows from

$$\Delta F^{o} = (\sum \Delta F_f)_{\text{products}} - (\sum \Delta F_f)_{\text{reactants}} \tag{3}$$

where all terms, except that pertaining to MB are known.

The success of this direct approach depends, of course, on how well the concentrations, indicated in Equation (2), can be determined, and how closely their ratio approaches that which actually obtains at equilibrium. This report is concerned with the solution of these problems in connection with the high temperature formation of sodium metaborate.

EXPERIMENTAL SYSTEM

The arrangement of experimental components is shown in Figure 1. The light source and 1.5 meter grating instrument constitute an absorption spectrometer for determining the concentration of free metal in the burner exhaust. The other monochromator measures light emission from the OH-radical, from which the H-atom concentration is inferred.

Absorption Spectrometer

The light source is an Osram sodium vapor, glow discharge lamp which emits only lines belonging to the spectrum of atomic sodium. Light radiated from the exhaust is rejected by tuning the photomultiplier circuit, with a Princeton Applied Research lock-in amplifier, to the chopping frequency of the lamp. The latter occurs naturally at 120 cps, since the lamp is operated from 60 cps line voltage. The reference frequency is provided by the output of a full-wave silicon rectifier. The above features assure that any change in light intensity can be unequivocally attributed to absorption by sodium vapor in the exhaust.

The exit slit passes both components of the sodium D-doublet. The output of the RCA IP-28 photomultiplier tube is shunted with a resistor, which, in conjunction with the aperture stop on the second lens, is adjusted to limit the tube output to 10 microamp, in accord with the manufacturers specification for linear performance. The aperture stop is always kept sufficiently small that the solid angle subtended by the flame does not exceed that from the source lamp. Although the subsequent filtering will

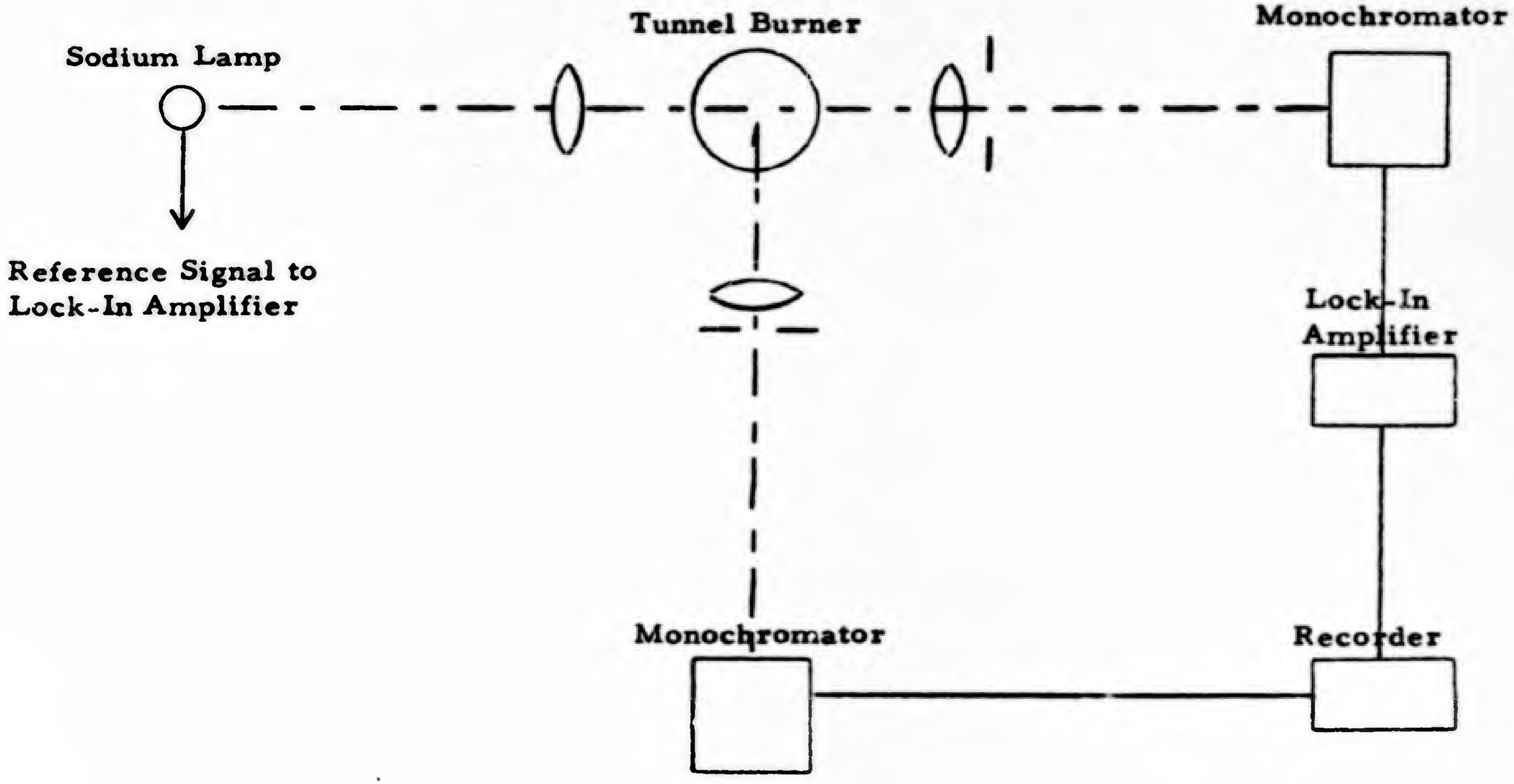

Figure 1. Block Diagram Of Experimental Arrangement.

not pass radiated light, this maximizes the signal contribution to the allowed 10 microamp output, and improves the sensitivity.

The signal is recorded on a Mosely Model 2D, X-Y recorder, using the time base for the X-axis.

Overall linearity of response to light intensity is checked by recording signals for various source intensities with and without a woven wire attenuator in the light path. The optical density of the attenuator is given by the Lambert-Beer relationship,

$$\log I_0/I = D \tag{4}$$

where I_0 pertains to the unattenuated light flux. The constancy of D was established within four percent over the experimental light intensity range. The variations in intensity are had by using other attenuators before the lamp, to vary I_0.

Tunnel Burner

The high temperature environment required for the reaction between sodium and the boron species was provided by a hydrocarbon flame in a tunnel burner, Figure 2. The interior of the burner is filled with a roaring, turbulent flame, providing thorough mixing of the sodium-containing gas, which enters axially, as indicated. The purpose of the burner extensions is to vary the gas residence time in the burner. If the flame is not too hot, the exhaust temperature can be maintained constant during this operation by the coiled Calrod heater. The burner is attached to a mount that allows it to be rotated out of the light path, for I_0 measurements, and returned to precisely the same position.

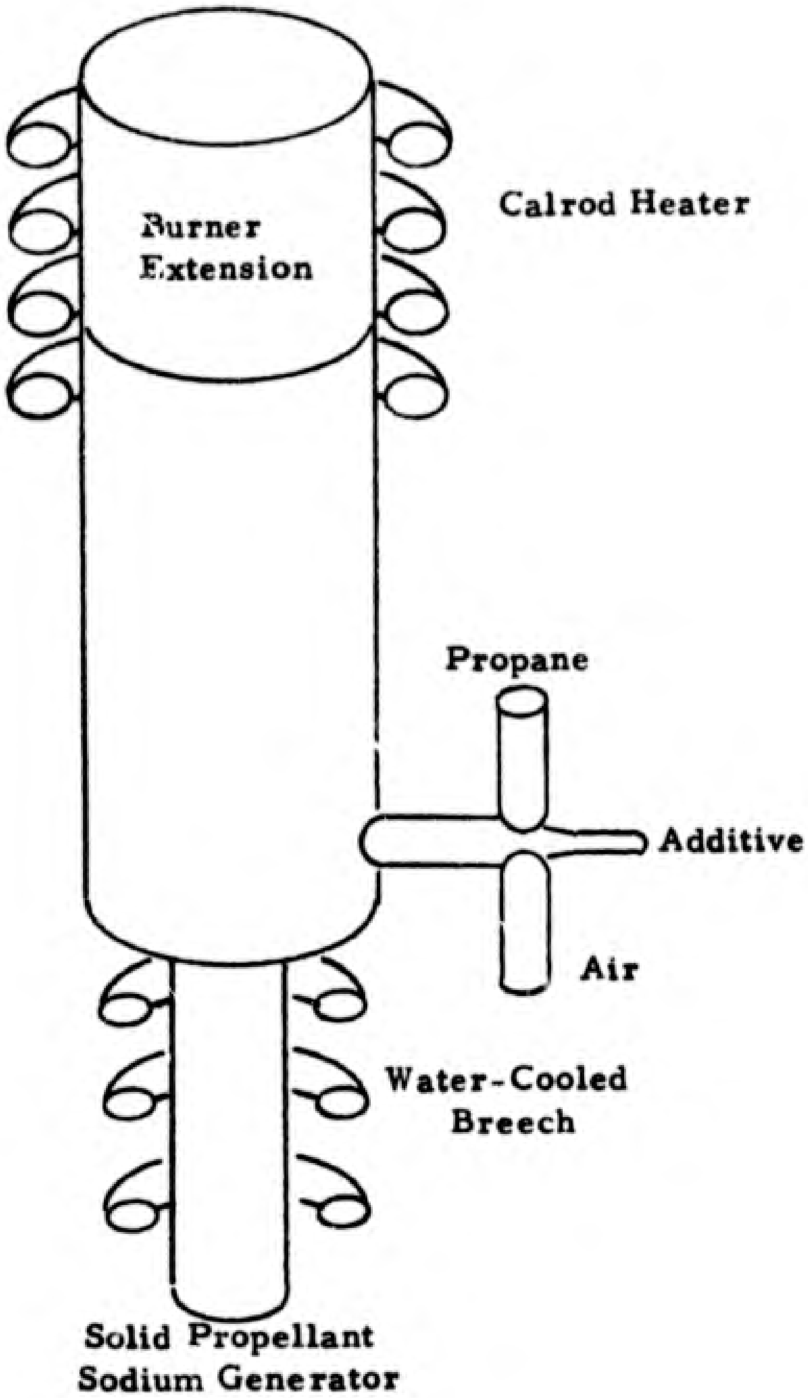

Figure 2. Tunnel Burner.

Mass Flows

The combustion gases, propane and air, are metered with variable-area flow meters, calibrated by positive displacement. The optical density measurements were found to be sensitive to small flow fluctuations, and the line air supply was smoothed with a Grove dome regulator.

The additives, boron trichloride and chlorine gas are metered with a Fisher-Porter Tri-Flat variable-area flowmeter. The reactive nature of these substances makes a positive displacement calibration difficult. These flows were calculated, using the procedure specified by the Fisher-Porter manual. The required viscosity data for boron trichloride was taken from Hawes, et al (1955).

Sodium vapor was introduced by utilizing the natural contamination of solid propellants with this material. The cylindrical strand, inhibited to insure end-burning, and contained in a disposable, mild steel tube, is inserted into the water-cooled burner breech. End ignition of the strand is effected by the burner flame. Sodium, homogeneously dispersed in the propellant as a natural contaminant, is directly emitted in the gas phase, eliminating the entrainment which is inherent in the use of an atomizer. Data demonstrating the reproducibility of mass flow and optical density (i.e. sodium flow) had with this solid generator are given in Table I.

The sodium mass-flow from the generator was determined by the analytical procedure known as "the method of additions". The strands, split lengthwise, are used to form a sandwich with a slip of filter paper, into which a precisely known amount of sodium has been absorbed. The optical densities in the burner exhaust, consequent to the burning of these strands, is used to construct a Beers Law working curve. The slope and intercept of this curve yield the sodium mass flow from the propellant, as described in detail elsewhere (Fleischer, 1963).

TABLE I

SODIUM-GENERATOR PERFORMANCE

Strand Length :	3.50 cm
Strand Weight*:	3.045 ± .014 (10)**g
Burning Time :	35.0 ± 0.6 (6) sec
Optical Density:	0.781 ± .002 (3)

---

* Includes 0.308 g of polyolefin inhibitor

** ( ) indicates number of replicates

Exhaust Characteristics

Extended measurements, required for temperature and sodium distribution profiles, do not require a knowledge of the sodium flow-rate. For this work a sodium boiler was more convenient than the strand generator, the latter being limited to a forty second operation time. The propellant generator contributes only five percent to the total flow, and its operation would not be expected to significantly alter the following results.

A sodium-line reversal temperature profile at the mouth of the burner is shown in Figure 3. The low spatial resolution, indicated by the larger of the scaled tungsten-lamp images, was an experimental error, but does not affect the shape of the profile.

Temperatures, reported later, pertaining to the thermochemical work are the results of point measurements made with the solid propellant sodium generator in operation. These were taken at the same position as the optical density measurements and had the same spatial resolution, indicated by the smaller image size of Figure 3.

An optical density profile is described by the data in Table II. The last column gives the optical density for a unit path length, corrected for the temperature incurred density variations. It is seen that the sodium concentration remains constant across the burner mouth within the experimental error in the optical measurements. These data were also generated with the sodium boiler. Aside from its convenience for extended measurements, the boiler has the particular advantage in this case, that the chlorine introduced by the solid propellant generator, is not present. Then, the only compound formed is a small amount of sodium hydroxide. Changes in the extent of its formation, effected by the temperature variation, will be correspondingly small, and the purpose of this experiment, to demonstrate uniform mixing of injected species with the main gas stream, is not obscured.

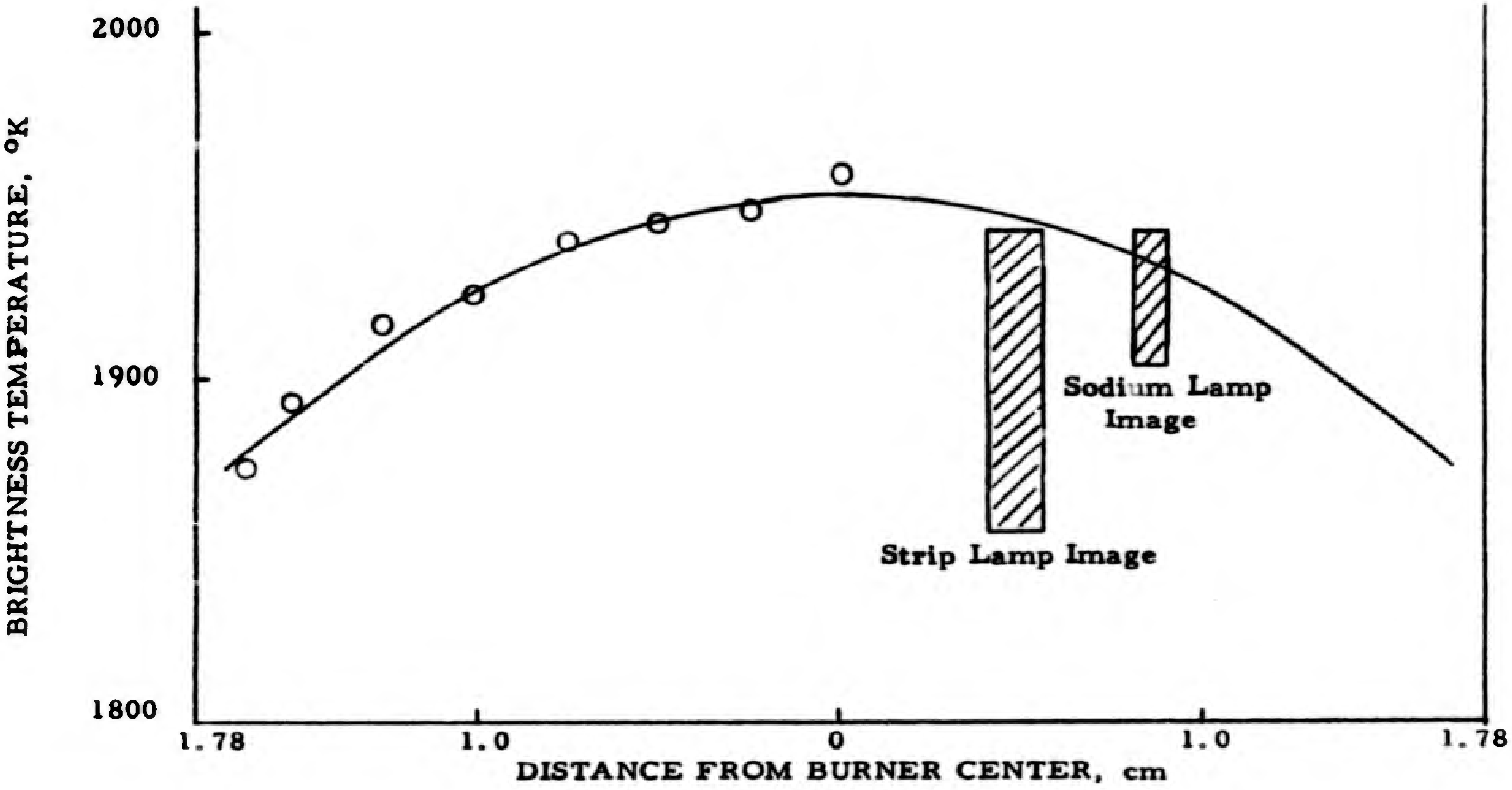

Figure 3. Temperature Profile Across Tunnel Burner.

TABLE II

OPTICAL DENSITY PROFILE ACROSS TUNNEL BURNER

Axial Displacement (cm)	L* (cm)	D	DT/LT_m** (cm^{-1})
0	3.56	.498	.140
.254	3.52	.498	.141
.508	3.42	.498	.145
.762	3.24	.489	.150
1.016	2.92	.429	.144
1.270	2.50	.373	.146
1.524	1.86	.270	.140
1.652	1.32	.229	.166
1.780	0	--	
			.146 ± .006

---

* Optical path length

** T_m is the maximum temperature measured. See Fig. 3

Flame Systems

Two propane-air flame systems, differing in their stoichiometries, were required. Although the sodium generator operates in a very reproducible fashion, the sodium content of different batches of propellant varies considerably. During the course of this work a new batch of propellant was required, which contained considerably more sodium than that previously used. The optical densities were reduced to a workable level by going to a leaner flame. These flames are described in Table III. Their equilibrium compositions are given in Tables IV and V. Only species whose concentrations will be later required are included.

TABLE III

FLAME SYSTEMS

Component	Flame I Mass Flows (g sec^{-1})	Flame II
Propane	.1026	.0864
Air	1.578	1.620
BF 122 Mod 1*	.082	.082
Polyethylene**	.0088	.0088
Chlorine	0.0 - 0.05	0.0 - 0.05
Boron Trichloride	0	0.0 - 0.04
Sodium	2.31×10^{-5}	6.52×10^{-5}
Conditions		
T (°K)	1930	1980
P (atm)	.987	.962

---

* Composition, gram atoms:

C	0.452
H	1.257
N	4.888
O	1.433
Mg	.0002
Cl	.0229
S	.0340

** Propellant inhibitor

TABLE IV

EQUILIBRIUM MOLE FRACTIONS, FLAME I

Chlorine added, 0

T (°K):	2015	1930*	1844
$\bar{M}$	28.0	28.0	28.0
HCl	.630 - 2	.635 - 2**	.639 - 2
Cl	.80 - 4	.40 - 4	0
H	.208 - 3	.136 - 3	.64 - 4
H_2O	.1609 + 0	.1605 + 0	.1601 + 0

Chlorine added, .01 g sec^{-1}

T (°K)	2021	1930*	1851
$\bar{M}$	28.1	28.1	28.1
HCl	.1064 - 1	.1073 - 1	.1080 - 1
Cl	.150 - 3	.80 - 4	0
H	.200 - 3	.126 - 3	.612 - 4
H_2O	.1592 + 0	.1587 + 0	.1584 + 0

---

* Interpolated

** $.635 \times 10^{-2}$

TABLE IV (Continued)

Chlorine added, .02 g sec^{-1}

T ($^{\circ}$K):	2027	1930*	1858
$\overline{M}$	28.2	28.2	28.2
HCl	.1496 - 1	.1510 - 1	.1520 - 1
Cl	.220 - 3	.150 - 3	.60 - 4
H	.193 - 3	.116 - 3	.59 - 4
H_2O	.1574 + 0	.1570 + 0	.1567 + 0

Chlorine added, .03 g sec^{-1}

T ($^{\circ}$K)	2032	1930	1864
$\overline{M}$	28.3	28.3	28.3
HCl	.1925 - 1	.1944 - 1	.1956 - 1
Cl	.310 - 3	.220 - 3	.90 - 4
H	.185 - 3	.107 - 3	.57 - 4
H_2O	.1556 + 0	.1552 + 0	.1549 + 0

Chlorine added, .05 g sec^{-1}

T ($^{\circ}$K):	2043	1930	1877
$\overline{M}$	28.5	28.5	28.5
HCl	.2775 - 1	.2808 - 1	.2823 - 1
Cl	.530 - 3	.410 - 3	.160 - 3
H	.171 - 3	.90 - 4	.52 - 4
H_2O	.1519 + 0	.1516 + 0	.1514 + 0

TABLE V

EQUILIBRIUM MOLE FRACTIONS, FLAME II

(Chlorine Added, .01 g)

T (°K):	1900	1980*	2000
$\overline{M}$	28.76	28.74	28.73
Cl	.479 - 3	.609 - 3**	.642 - 3
HCl	.1036 - 1	.1023 - 1	.1020 - 1
H	.0993 - 4	.2793 - 4	.324 - 4
OH	.0737 - 2	.1141 - 2	.1242 - 2
H_2O	.1482 + 0	.1477 + 0	.1476 + 0
(Chlorine Added, .02 g)			
$\overline{M}$	28.83	28.81	28.80
Cl	.693 - 3	.880 - 3	.927 - 3
HCl	.1458 - 1	.1438 - 1	.1433 - 1
H	.0966 - 4	.272 - 4	.316 - 4
OH	.0745 - 2	.1151 - 2	.1252 - 2
H_2O	.1455 + 0	.1451 + 0	.1451 + 0

---

* Interpolated

** .609 x 10^{-3}

TABLE V (Continued)

(Chlorine Added, .03 g)

T (°K):	1900	1980*	2000
$\overline{M}$	28.88	28.86	28.85
Cl	.0916 - 2	.1162 - 2	.1224 - 2
HCl	.1877 - 1	.1851 - 1	.1844 - 1
H	.0941 - 4	.265 - 4	.308 - 4
OH	.0751 - 2	.1160 - 2	.1262 - 2
H_2O	.1430 + 0	.1426 + 0	.1425 + 0
(Chlorine Added, .04 g)			
$\overline{M}$	28.93	28.94	28.94
Cl	.1147 - 2	.1454 - 2	.1531 - 2
HCl	.239 - 1	.228 - 1	.225 - 1
H	.0918 - 4	.259 - 4	.301 - 4
OH	.0756 - 2	.1168 - 2	.1271 - 2
H_2O	.1404 + 0	.1402 + 0	.1402 + 0

EQUILIBRIUM?

The validity of the results found in this work depends upon how closely the ratios of metal-containing species approach their equilibrium value. A direct test of equilibrium was made by measuring the optical density of sodium in the burner exhaust as a function of residence time. This was accomplished by varying the burner length, while the exhaust temperature was maintained constant with a Calrod heater wrapped around the burner. Some typical results are:

TABLE VI

EFFECT OF RESIDENCE TIME ON SODIUM CONCENTRATION

Burner Length (cm)	Δt (sec)	Optical Density
7.1		.69 ± .01 (4)*
	2.0×10^{-3}	
8.1		.57 ± .02 (3)
	4.0×10^{-3}	
10.1		.54 ± .01 (3)

---

* number of replicates

The 8.1 cm length is the one used for the thermochemical studies, and while the density measurement has largely stabilized at this point, the small decrement found upon going to 10.1 cm is real.

In the next section, the measurement of free-radical concentration in these systems is described. These measurements also indicated a departure from equilibrium, much more conclusively than for the sodium species. Sugden has shown that free radical species are in quasi-equilibrium in hydrogen flames, and Reid and Wheeler (1961) have applied similar arguments to propane-air flames. At this point in this investigation the possibility was considered that the non-equilibrium behavior of the sodium species was a direct reflection of the decaying free radical excess, and that the sodium reactions were also in quasi-equilibrium. Indeed, this argument has already been propounded by Sugden for hydrogen-air flames (Bulewicz, James and Sugden, 1956).

To proceed with our argument, we must further anticipate results given in more detail later. Optical absorption coefficients, which are atomic constants, determined for sodium in both Flames I and II, are in excellent agreement. The extraction of these coefficients requires equilibrium expressions, and since these flames differ markedly in their free-radical content, the experimental agreement strongly supports the quasi-equilibrium arguments.

HYDROGEN ATOM CONCENTRATION

The concentrations of metal compounds, in this work, are described in terms of equilibrium constants, all of which contain the concentration of H-atom. Since free radicals are often out of equilibrium in flames, an experimental determination is required.

In the present work it is sufficient if the free-radical measurement yields relative concentrations. These were found by measuring light emission from the burner exhaust, at the 3067Å OH-band, as a function of additive flow-rate. Light emission is related to species concentration by the expression

$$I = B \left[1 - \exp(-aCL)\right] \tag{5}$$

a	absorption coefficient
C	concentration
L	optical path length

where the constant, B, contains atomic, geometric and instrument factors. If

$$1 - \exp(-aCL) \doteq aCL \tag{6}$$

the system is optically thin, and the intensity of light emission is directly proportional to the concentration of emitters. The absorption coefficient

$$a = 1.03 \times 10^{-19}\ \text{cm}^2$$

was calculated from Benedict and Plyler's (1954) absorption f-number for the 3067Å, $^2\Pi \rightarrow {}^2\Sigma$, (0,0)-band. The maximum probable OH-concentration was had by increasing the calculated equilibrium value by a factor of ten, in accord with Reid and Wheeler's (1961) findings in propane-air flames. The results are 0.023 and 0.024 for the left- and right-hand members of Equation (6).

According to the quasi-equilibrium relation between free radicals

$$\frac{(H)}{(OH)} = \frac{(H)_e}{(OH)_e} \tag{7}$$

where sub-e pertains to equilibrium conditions. In the present work the water concentration remains constant with changing additive flow-rate, and it is convenient to express $(OH)_e$ in terms of the equilibrium constant

$$K = \frac{(H)(OH)}{(H_2O,} \tag{8}$$

The H-atom concentration is then given by

$$(H) = b_1 \, (H)_e{}^2 \, I_{OH} \tag{9}$$

where the constant, b_1, contains B and K.

The experimental results are shown in Figures 4-6, where equilibrium calculations predict increases, with additive flow, of OH-concentration in all cases.

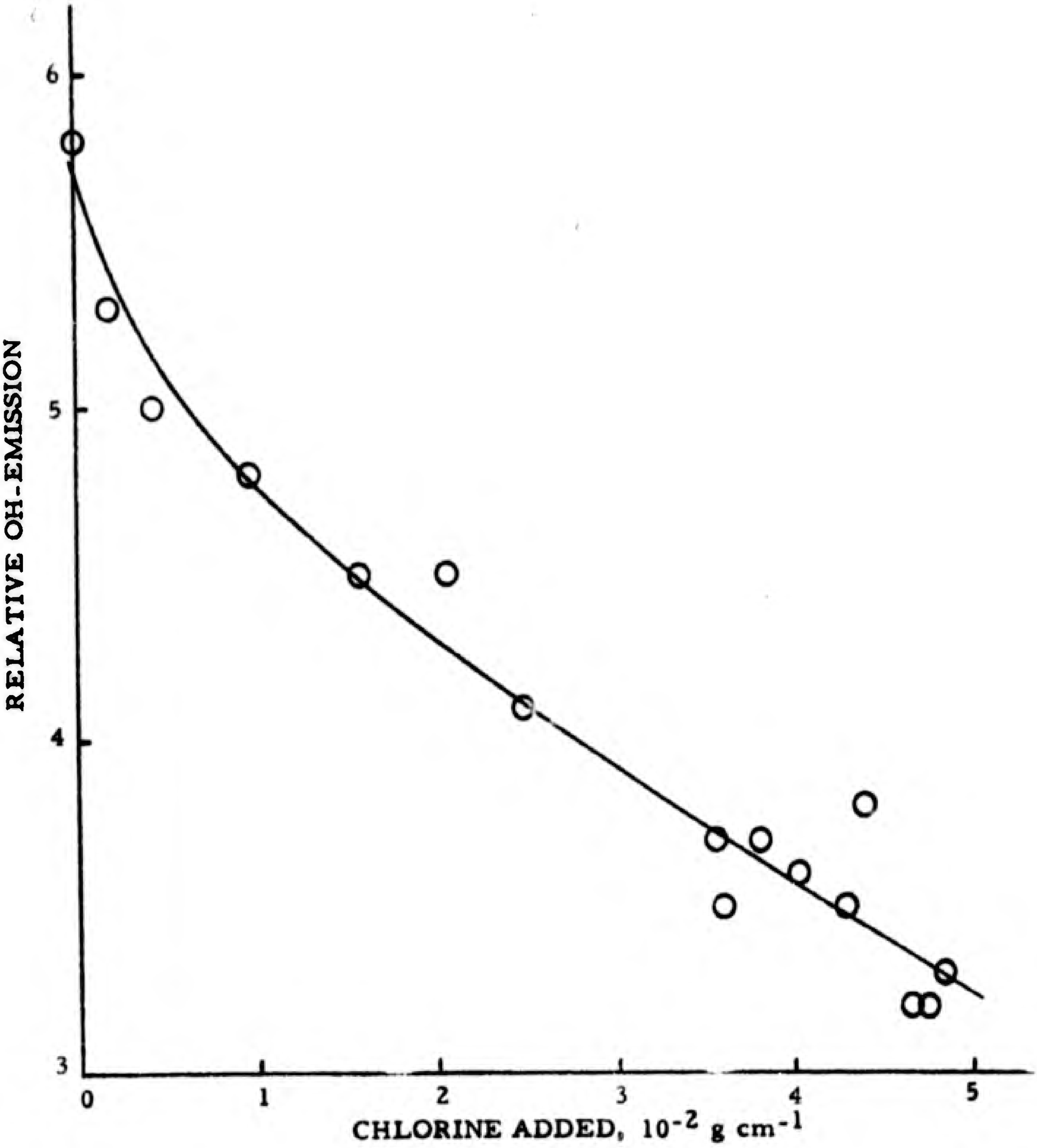

Figure 4. Effect Of Chlorine On 3067 Å OH-Emission, Flame I.

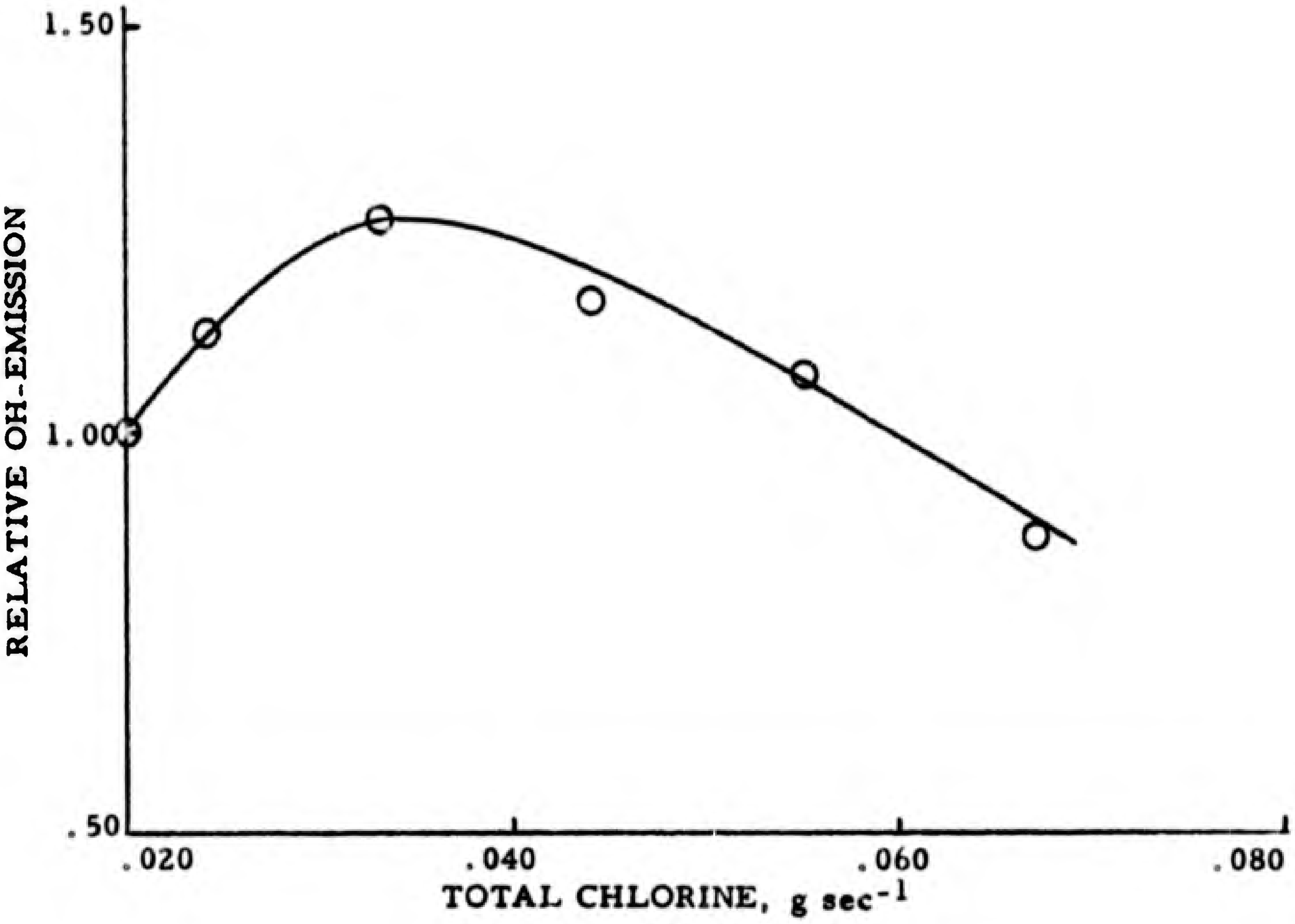

Figure 5. Effect of Chlorine On 3067 Å Emission, Flame II.

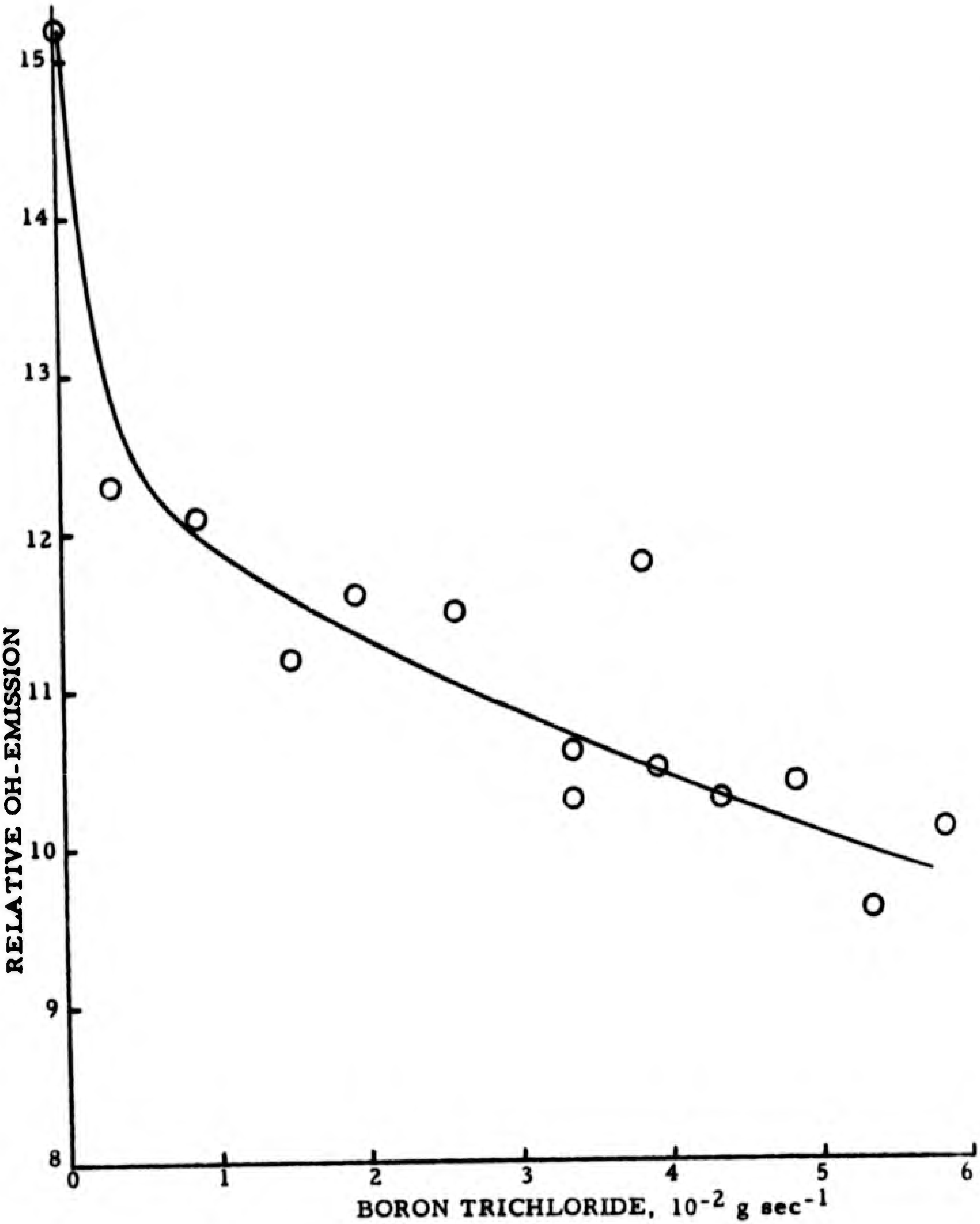

Figure 6. Effect Of Boron Trichloride On 3067 Å OH-Radiation, Flame II.

THE ABSORPTION COEFFICIENT

Analysis

In an environment such that only sodium chloride and sodium hydroxide can be formed, the materials balance for sodium is given by

$$T_{Na} = Na + NaCl + NaOH \qquad (10)$$

The compound concentrations can be expressed in terms of the equilibrium constants, K, for the reactions

$$Na + HCl = NaCl + H,\ K_1 \qquad (11)$$

$$Na + H_2O = NaOH + H,\ K_2 \qquad (12)$$

yielding

$$(NaCl) = K_1 \frac{(Na)(HCl)}{(H)} \qquad (13)$$

$$(NaOH) = K_2 \frac{(Na)(H_2O)}{(H)} \qquad (14)$$

Inserting these relations into Equation (10)

$$K_1 \frac{(HCl)}{(H)} = \frac{T_{Na}}{(Na)} - 1 \qquad (15)$$

since examination of the relative magnitudes of K_1 (HCl) and K_2 (H_2O) indicates that the latter term can be dropped. If total chlorine is small compared to total hydrogen, the concentration of hydrogen chloride is linearly related to the chlorine flow

$$(HCl) = b_2 \dot{m}_{Cl} \qquad (16)$$

The hydrogen atom concentration is derived from the quasi-equilibrium relationship between calculated H-atom concentration and the 3067Å hydroxyl intensity, I_{OH}, as described above

$$(H) = b_1 (H)_e^2 I_{OH} \tag{9}$$

The free sodium concentration, according to the Lambert-Beer relationship, is proportional to the optical density

$$(Na) = cD \tag{17}$$

Combining Equations (9) and (15-17)

$$\frac{\dot{m}_{Cl}}{(H)_e^2 I_{OH}} = \left[\frac{b_1 T_{Na}}{b_2 K_1 c}\right] \frac{1}{D} - \frac{b_1}{b_2 K_1} \tag{18}$$

Experimental Results

Chlorine was metered into the tunnel burner with the solid-propellant sodium injector in operation. The optical density at the sodium D-line, and the emitted intensity at the 3067Å OH-band were recorded. The data for Flames I and II are given in Tables VII and VIII. The entries under I_{OH}, the emitted intensity at the 3067Å OH-band, were interpolated from Figures (4) and (5), above. The equilibrium H-atom mole fractions, $(H)_e$, were graphically interpolated from the data of Tables IV and V, above. These data, represented according to Equation (18) are shown in Figures (7) and (8). In Table VII the seven data, having reciprocal densities larger than 3.5, exhibit marked scatter and are greatly displaced in a positive direction on the ordinate of Figure (7). These points are not included in this figure.

TABLE VII

EFFECT OF CHLORINE ON FLAME I

Run	Chlorine 10^{-2} g sec^{-1}	D^{-1}	I_{OH}*	$(H)_e$ (10^{-5})	$\dot{m}_{Cl}/(H)_e^2 I_{OH}$ (10^{-2})
414	6.87	4.44	3.31	9.06	2.52
403	6.73	4.31	3.37	9.20	2.36
401	6.63	3.89	3.39	9.26	2.28
415	6.60	4.33	3.40	9.30	2.24
394	6.55	3.91	3.42	9.35	2.19
412	6.12	3.76	3.55	9.69	1.83
404, 411	5.90	3.76	3.62	9.89	1.66
398	5.18	3.40	3.87	10.5	1.22
391	5.00	3.48	3.93	10.7	1.11
409	4.45	2.92	4.14	11.2	.86
399, 406	4.07	2.34	4.27	11.5	.72
400	4.02	2.38	4.30	11.6	.69
395	3.72	2.28	4.42	11.9	.60
413	3.41	2.13	4.57	12.2	.50
405	3.37	1.98	4.58	12.2	.48
396, 397	2.73	1.74	4.94	12.9	.33
392	2.50	1.62	5.10	13.1	.29
393	2.43	1.58	5.16	13.2	.27
407, 408, 416	2.19	1.41	5.39	13.4	.23
410, 417, 418	2.00**	1.28	5.71	13.6	.19

---

* Arbitrary units

** From solid propellant

TABLE VIII

EFFECT OF CHLORINE ON FLAME II

Run	Chlorine (10^{-2} g sec^{-1})	D^{-1}	I_{OH}*	$(H)_e$ (10^{-5})	$\dot{m}_{Cl}/(H)_e^2 I_{OH}$
315-19	2.00**	1.98	1.00	2.86	.245
320	2.38	2.54	1.11	2.83	.267
321	2.98	3.61	1.23	2.79	.311
327	3.63	4.46	1.26	2.75	.381
328	3.63	4.10	1.26	2.75	.381
323	3.76	4.69	1.25	2.74	.401
322	3.95	5.56	1.24	2.73	.428
326	4.33	4.74	1.21	2.70	.491
324	4.75	6.29	1.16	2.67	.574
325	5.67	8.85	1.04	2.61	.800

---

* arbitrary units

** from solid propellant

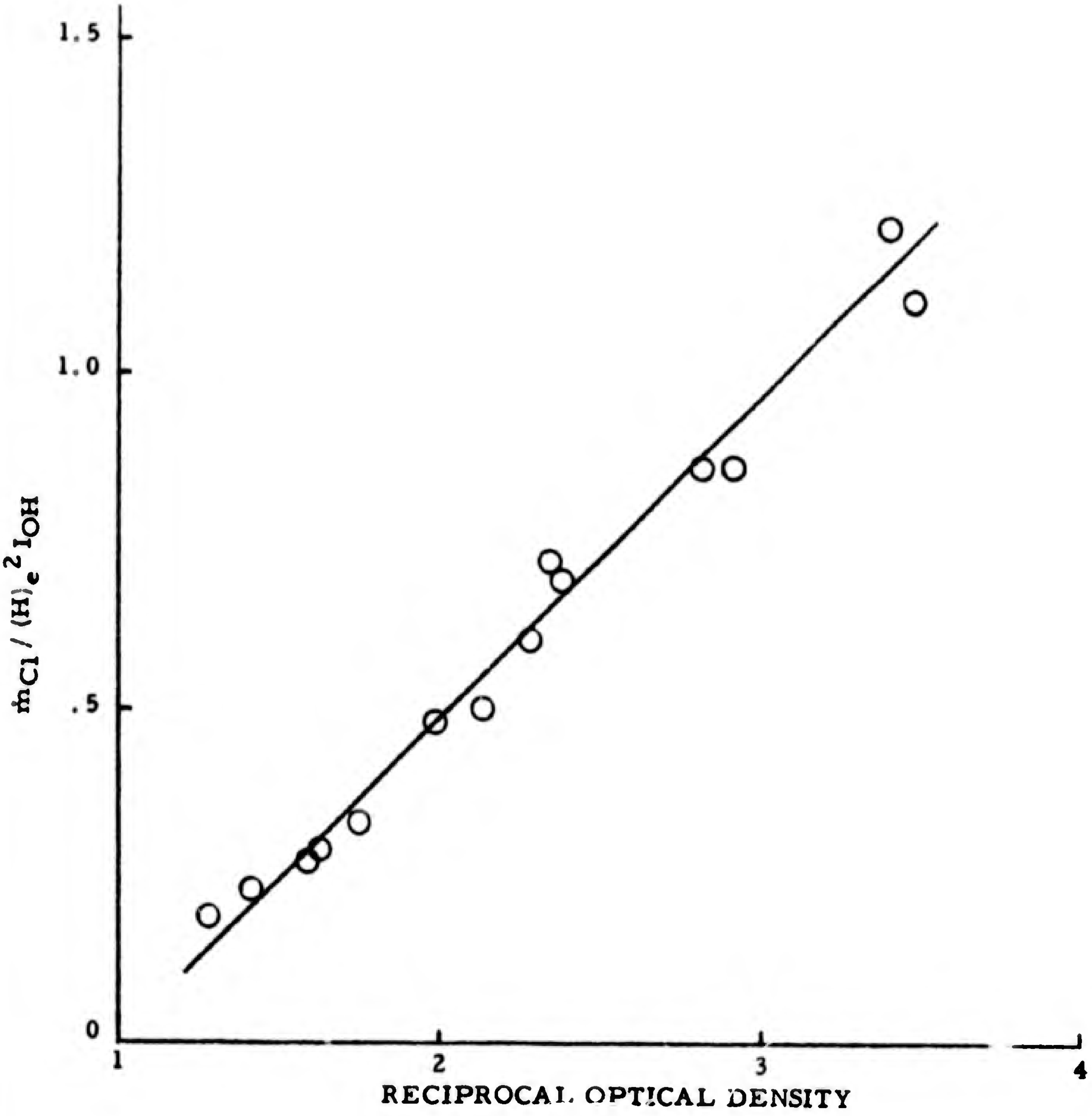

Figure 7. Determination Of The Absorption Coefficient, Flame I.

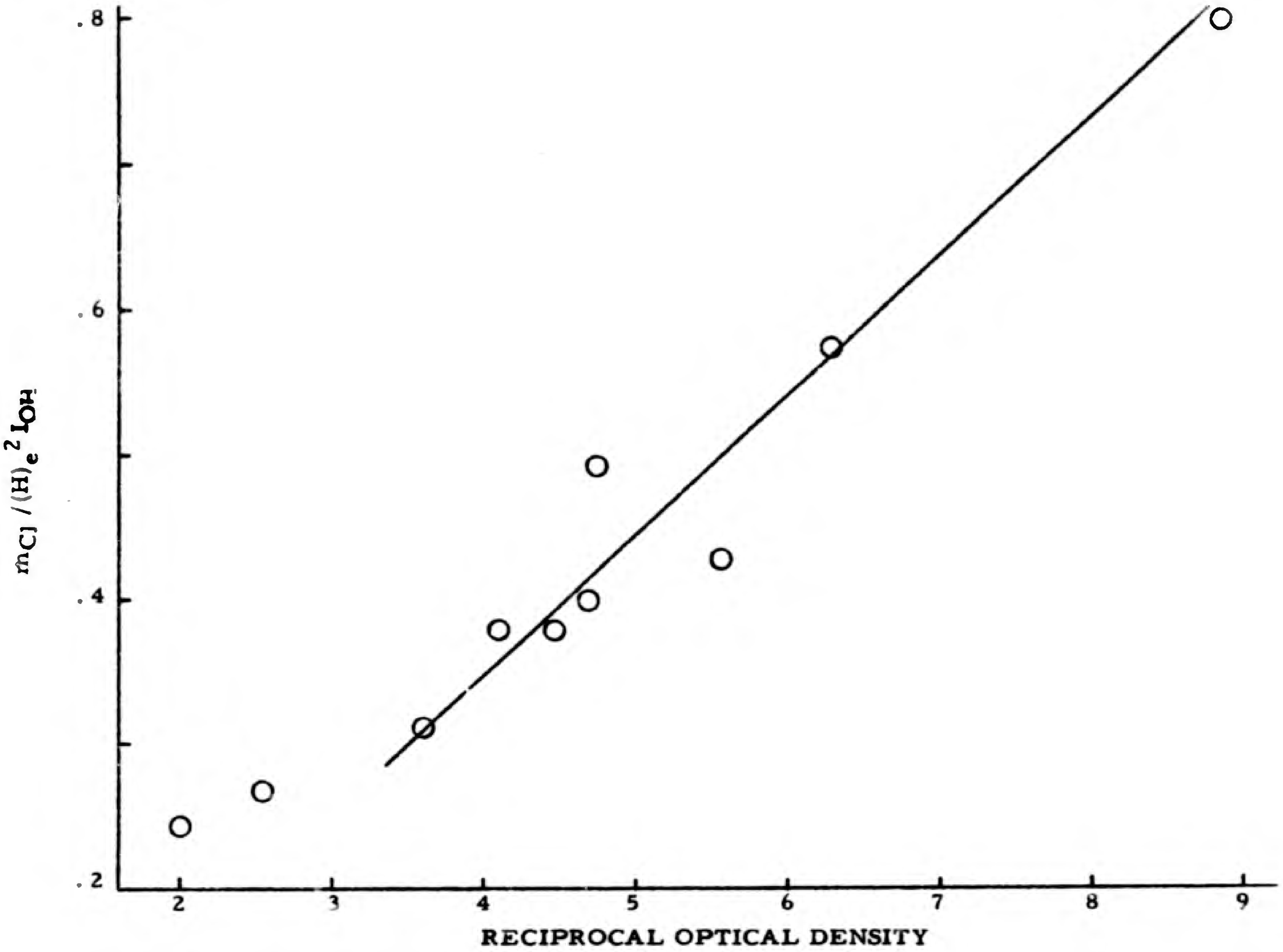

Figure 8. Determination Of The Absorption Coefficient, Flame II.

From the slopes and intercepts of Figures (7) and (8), the following values of the coefficient, c, are derived.

	Slope	Intercept	T_{Na}	$\underline{c}$
Flame I :	0.48	-0.47	1.59×10^{-5}	1.56×10^{-5}
Flame II:	0.96	-0.36	4.51×10^{-5}	1.68×10^{-5}

The coefficient, c, pertains to concentrations on a mole fraction basis. The absorption coefficient, a, based on number density and unit path length can be had from the expression

$$a = \frac{RT}{PLc} \tag{19}$$

R	gas constant
T	absolute temperature
P	absolute pressure
L	optical path length

The following data

Flame	T (°K)	P (torr)	L (cm)
I	1930	750	3.0
II	1980	730	3.0

yield

$$a = 3.6 \pm 0.2 \times 10^9 \text{ cm}^2 \text{ mole}^{-1}$$

and the agreement between the results from the two flame systems is quite satisfactory.

FORMATION OF SODIUM METABORATE

The effects of adding chlorine and boron trichloride on the optical density of sodium in the burner exhaust were compared as a function of total chlorine flow. It is apparent that the increased decrement in the optical densities caused by boron trichloride must be effected by the formation of some compound other than sodium chloride or sodium hydroxide.

Boron Compounds

The identity of the boron reactant was derived from an examination of the relative concentrations of the boron species. These were estimated by combining JANAF (1960) free-energy data with the calculated equilibrium concentrations of hydrogen, oxygen and chlorine in the experimental system, Flame II. The procedure is summarized by

$$B' + mH_2 + nO_2 + pCl_2 = B'' \qquad (20)$$

$$\frac{(B'')}{(B')} = \frac{K''}{K'} (H_2)^m (O_2)^n (Cl_2)^p \qquad (21)$$

where B' and B" are two boron species containing any quantity, including zero, of H, O, Cl. The K's are equilibrium constants derived from the free-energies of formation of the two compounds. The results, Table (IX), indicate that almost the entirety of boron exists as metaboric acid, with a small contribution from boron dioxide. This result also indicates that the sodium-boron compound being formed is the metaborate, $NaBO_2$. This choice is supported by the chemical literature, which indicates no other Na-B-O compound.

TABLE IX

CONCENTRATIONS OF BORON SPECIES IN FLAME II

Species	Relative Concentration
HBO_2	0.935
BO_2	0.064
H_3BO_3	2.8×10^{-4}
HBO	4.7×10^{-5}
BOCl	3×10^{-5}
BO	2×10^{-6}
BCl_2	2×10^{-12}
BCl_3	2×10^{-12}
BCl	1×10^{-15}
B	$< 10^{-15}$
B_2O_3	$< 10^{-15}$
All	1.0000

Analysis

The formation of sodium metaborate is expressed in terms of the equilibrium constant of the reaction

$$\mathrm{Na} + \mathrm{HBO_2} = \mathrm{NaBO_2} + \mathrm{H}, \; K_3 \qquad (22)$$

yielding for its concentration

$$(\mathrm{NaBO_2}) = K_3 \frac{(\mathrm{Na})(\mathrm{HBO_2})}{(\mathrm{H})} \qquad (23)$$

The materials balance for sodium then yields

$$\frac{T_{\mathrm{Na}} - (\mathrm{Na})}{(\mathrm{Na})} = K_1 \frac{(\mathrm{HCl})}{(\mathrm{H})} + K_3 \frac{(\mathrm{HBO_2})}{(\mathrm{H})} \qquad (24)$$

The sodium concentration is found from the optical density

$$(\mathrm{Na}) = cD$$

where c is the experimentally determined value, as described above. The hydrogen chloride derives from the chlorine contained in the solid-propellant sodium generator, as well as from the chlorine content of the BCl_3 additive. Its mole fraction is given by

$$(\mathrm{HCl}) = \frac{\overline{M}\, \dot{m}_o}{M_{Cl}\, \dot{m}_T} + 0.908 \frac{\overline{M}\, \dot{m}_B}{M_{Cl}\, \dot{m}_T} \qquad (25)$$

$\overline{M}$	average molecular weight
$\dot{m}_o$	propellant chlorine flow
$\dot{m}_T$	total mass flow
$\dot{m}_B$	BCl_3 mass flow

Similarly, the metaboric mole fraction is

$$(\mathrm{HBO_2}) = 0.0922 \frac{\overline{M}\, \dot{m}_B}{\overline{M}_B\, \dot{m}_T} \qquad (26)$$

where M_B is the molecular weight of boron trichloride. The H-atom concentration is given by

$$(H) = b_1 \, (H)_e^2 \, I_{OH} \tag{9}$$

as described above.

Defining the following constants

$$b_2 \equiv \frac{K_1 \overline{M}}{M_{Cl} \, \dot{m}_T} \tag{27}$$

$$b_3 \equiv .0922 \, \frac{K_3 \overline{M}}{M_B \, \dot{m}_T} \tag{28}$$

Equation (**24**) becomes

$$\frac{T_{Na} - cD}{cD} (H)_e^2 \, I_{OH} = \left[.908 \frac{b_2}{b_1} + \frac{b_3}{b_1} \right] \dot{m}_B + \frac{b_2}{b_1} \dot{m}_o \tag{29}$$

Experimental Results

Flame II was used for this work. The effect of boron trichloride on the sodium concentration is shown in Figure 9. Smoothed data, from this figure, are entered in Table X, where the calculated ordinates of Equation (29) are indicated "y" in the last column.

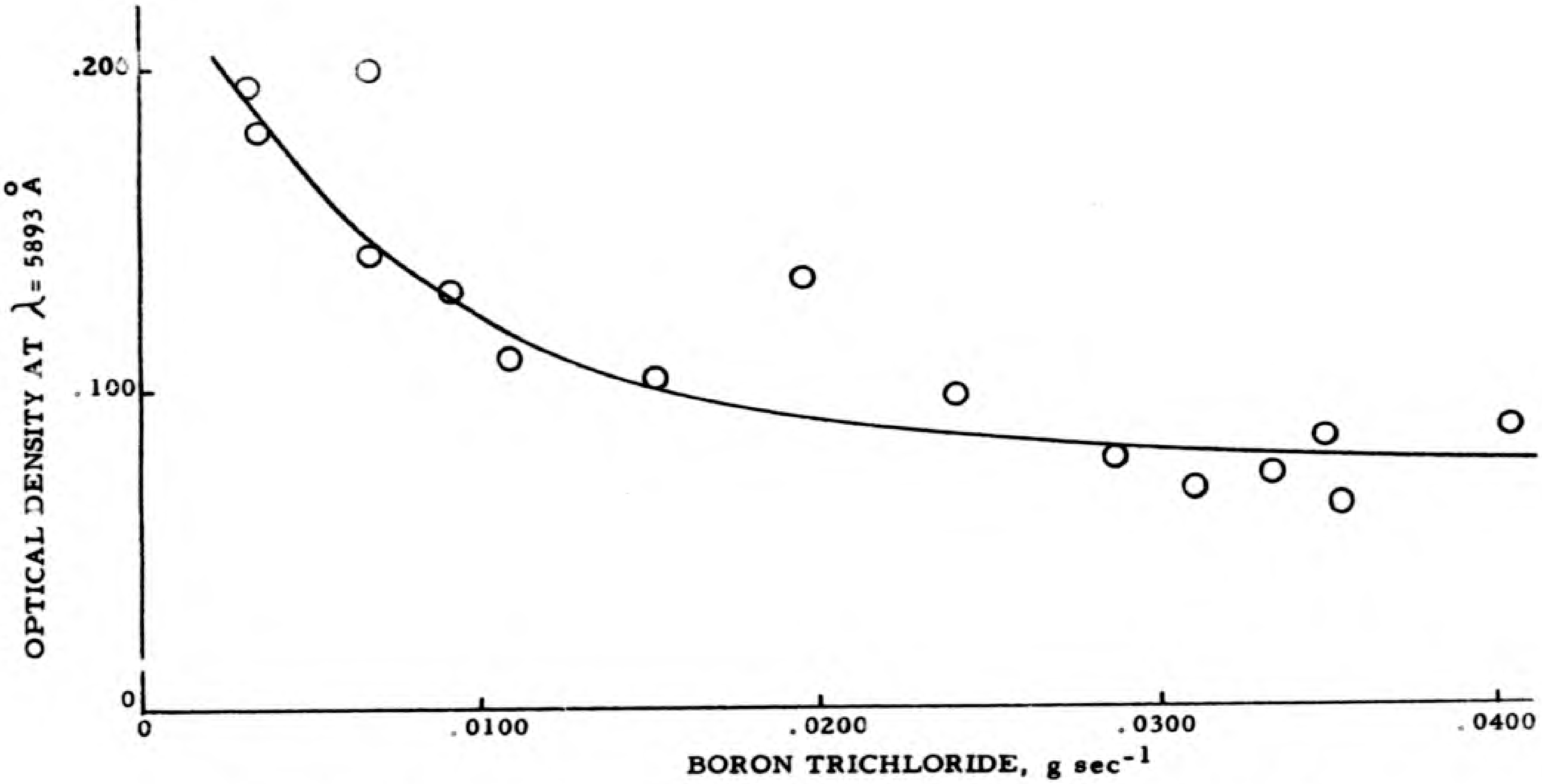

Figure 9. Effect Of Boron Trichloride On The Sodium Concentration In Flame II.

TABLE X

EFFECT OF BORON TRICHLORIDE ON FLAME II

$T_{Na} = 4.51 \times 10^{-5}$, $c = 1.68 \times 10^{-5}$

BCl_3 $(10^{-3}$ g sec$^{-1})$	D	I_{OH}*	$(H)_e$** (10^{-5})	y (10^{-7})
3	.195	12.9	2.84	1.32
4	.179	12.6	2.83	1.40
5	.166	12.4	2.83	1.50
6	.155	12.3	2.82	1.60
7	.145	12.2	2.81	1.68
8	.137	12.1	2.81	1.78
9	.130	12.0	2.80	1.86
10	.123	11.9	2.80	1.95
12	.112	11.8	2.78	2.11

---

* Interpolated from Figure 6.

** Graphically interpolated from Table V data.

From the graphical solution of Equation (29), shown in Figure 10, the following values are had

$$.908\frac{b_2}{b_1}+\frac{b_3}{b_1}=8.82\times 10^{-2}$$

$$\frac{b_2}{b_1}\dot{m}_o=1.06$$

where the chlorine from the propellant, $\dot{m}_o = 2.00 \times 10^{-2}$ g sec^{-1}. Utilizing Equations (27) and (28), the equilibrium constant for the exchange reaction

$$NaCl + HBO_2 = NaBO_2 + HCl \tag{30}$$

is determined to be

$$K_3/K_1 = 2.50$$

from which the free-energy of formation, ΔF_f, for sodium metaborate can be derived, if one is willing to accept the published thermochemical data pertaining to the other species.

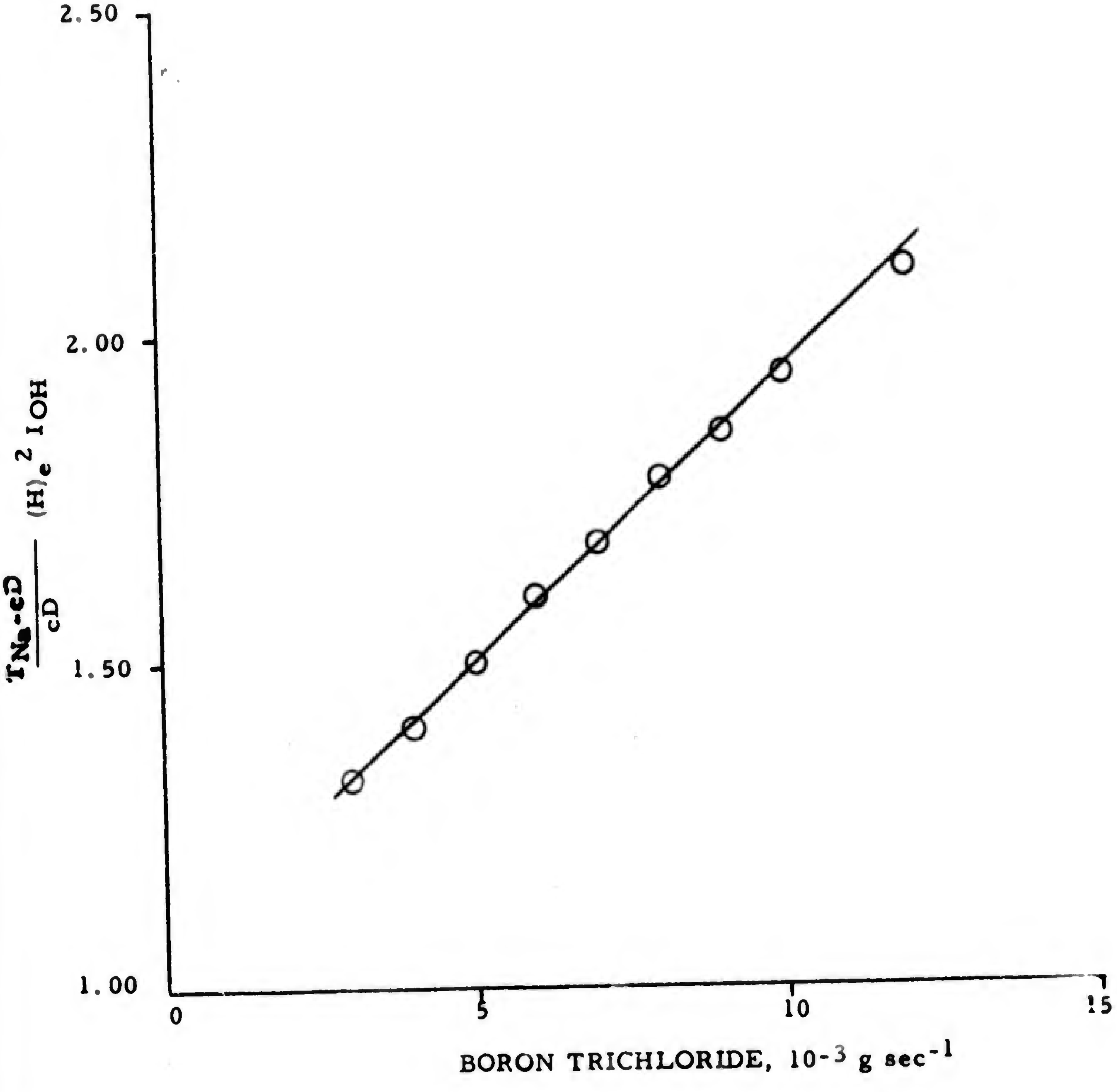

Figure 10. The Formation Constant Of Sodium Metaborate.

DISCUSSION

There are two important points on which this work can be criticized: the quasi-equilibrium assumption and the lack of positive identification of the sodium-boron adduct. The second of these, since it cannot be effectively answered, is easily, if not satisfactorily, disposed of. Only one piece of evidence concerning the possible nature of this compound can be extracted from the experimental results. If it is indeed formed by the replacement of an H-atom in a boron species by sodium, then, only the formation of the mono-sodium compound is consistent with the data.

In principle, of course, further conclusions of this nature can be made. An examination of the possible boron species, Table IX, indicates their dependence on the partial pressures of hydrogen and oxygen. Thus a comparison of the results of data reduction schemes, where reactants other than HBO_2 and products other than $NaBO_2$ are considered should reveal the true mechanism. It is amply clear, however, that the present data are not sufficiently precise for this purpose.

A much better justification can be made for assuming quasi-equilibrium. As noted above, the OH-intensity measurements are a definite indication of free-radical non-equilibrium, and as such, open the possibility that the sodium non-equilibrium relates to this, rather than to a slowness in the sodium reactions. A very positive affirmation of this is found in the good agreement of the two absorption coefficients found in environments differing markedly in their free-radical concentrations.

Some further mention of the OH-measurements in Flame II, in the presence of chlorine (Figure 5), must be made. It is noted that the OH-intensity increases with small, increasing chlorine flow, but then decreases as the flow becomes larger. No explanation for this phenomenon comes to mind.

REFERENCES

HAWES, J., A. E. Mackenzie and C. J. G. Raw. 1955. J. South African Chem. Inst. 8 21-24; cf, CA 50 15204 e (1956).

FLEISCHER, D. 1963. "Solid propellant tracing methods", Thiokol Chemical Corp., Reaction Motors Division Report RMD 5510-S, Office of Aerospace Research Contract AF 49(638)-1197.

REID, R. and R. Wheeler. 1961. "Hydrogen atom excesses in some propane flames". J. Phys. Chem. 65 527-30.

BULEWICZ, E. M., C. G. James and T. M. Sugden. 1956. "Photometric investigation of alkali metals in hydrogen flame gases, Part II". Proc. Roy. Soc. (London) A235 89-106.

BENEDICT, W. S. and E. K. Plyler. 1954. "High resolution spectra of hydrocarbon flames" in Energy transfer in hot gases. NBS Circular No. 523, Washington, D. C.

JANAF INTERIM THERMOCHEMICAL TABLES. 1960. The Dow Chemical Company, Midland, Michigan.